79-4047

Aiming an Electromagnetic Beam by Bending Segments of a Large Reflecting Surface

David Bushnell*
Lockheed Palo Alto Research Laboratory, Palo Alto, Calif.

Formulas are derived for initial and residual root-mean-squared (rms) surface shape error and edge moments and force amplitudes for a deformable primary reflecting surface composed of an array of relatively small diameter circular elements. These formulas apply to the reshapement of large shallow primary reflectors in such a way that the reflector at the focus of the primary (the secondary) does not move. The edge moment and force resultants required to minimize the rms residual surface error of each circular element of the primary are derived for $n=0$ and $n=1$ circumferential waves from a shallow shell theory published by Reissner in 1946 and for $n\geq 2$ circumferential waves from an inextensional bending theory published by Flügge in 1960. It is found that for reasonable configurations most of the residual rms surface error is axisymmetric and proportional to the square of the diameter-to-thickness ratio of the circular elements. The formulas demonstrate clearly that sandwich wall construction is superior to monocoque, permitting the use of thinner, lighter shells and smaller actuation forces and moments.

Nomenclature

ber,bei = Kelvin functions of order zero. (see Ref. 10)
C = extensional rigidity, Eq. (45a)
c = $\cos\alpha$
D = primary array diameter
d = circular element diameter
E = Young's modulus of wall material in face sheets of sandwich
E_n = residual rms surface error in circular element corresponding to n circumferential waves
E_{In} = initial rms error in circular element for n circumferential waves
E_I = initial rms error in entire primary array
E_r = residual rms error in entire primary array
e = ratio of face sheet thickness to total thickness, $e=t_{\text{face}}/t$
F = stress function, defined in Ref. 2
f = primary array f number: $f=R/(2D)$
$g_n(r)$ = coefficients of trigonometric expansion of initial error, $w_r(r,\theta)$
I_i,J_i = Bessel functions of order i (see Ref. 10)
i = $(-1)^{1/2}$
$\bar{i},\bar{j},\bar{k}$ = unit vectors associated with the x,y,z axes, respectively
$\bar{i}'',\bar{j}'',\bar{n}$ = vectors (not unit) associated with x'',y'',z'' axes, respectively; Eqs. (11, 13, and 7)
K = flexural rigidity, Eq. (45b)
k = Reissner number, Eq. (44); $k^4=C(1-\nu^2)/(KR^2)$
ℓ_i,m_i,n_i = direction cosines as defined by Eqs. (6) and (14)
M = (edge moment)/(circumferential arc length) of circular element, Fig. 5
$M_{r\theta}$ = (twisting moment)/(arc length) of circular element
N = (meridional stress resultant)/(circular arc length), Fig. 5
n = number of circumferential waves around circumference of circular element
q = quantity defined in Eq. (28)
Q = transverse shear force resultant at edge of circular element
R = radius of curvature of the circular elements before reshapement
r,θ = polar coordinates for circular element, Figs. 3 and 5
r_0 = radius of circular element, Fig. 5
s = $\sin\alpha$
t = shell wall thickness; for sandwich $t=2t_{\text{face}}+t_{\text{core}}$
V = (normal force)/(circumferential arc length) of circular element, Fig. 5; $V=Q+(\partial M_{r\theta}/\partial\theta)/r$
w_r = displacement distribution in z'' direction required for reshaping the circular spherical element to a part of a paraboloid, Fig. 2
w = displacement distribution in z'' direction due to edge loads on circular element
x,y,z = coordinate system attached to the apex of the primary array before reshapement or retargeting, Fig. 2
x',y',z' = coordinate system attached to apex of the paraboloidal retargeted primary array, Fig. 2
x'',y'',z'' = coordinate system attached to circular element, the apex of which lies on the retargeted primary array, as shown in Fig. 3
Y,Z = defined by Eqs. (4)
$y_0.z_0$ = coodinates, in x,y,z system, of apex of retargeted paraboloid
y = variable used in asymptotic expansion of Bessel functions, Eqs. (58), $y\equiv z^2/4$
z = complex variable; argument of Bessel functions; $z\equiv(i)^{1/2}kr$
y_c',r_c' = defined in Eqs. (23a) and (23b) and Fig. 4
α = retargeting angle
β = angle defined in Fig. 6
η,η^* = quantities defined in Eqs. (74) and (75)
λ = wavelength of electromagnetic radiation
ν = Poisson's ratio of wall material
ϕ = polar angle in circular segment, Fig. 5
ρ = density of wall material
θ = circumferential coordinate in circular element, Figs. 3 and 5

Subscripts

c = pertaining to centroid or apex of circular element
core = core of sandwich wall

Received March 3, 1978; revision received Sept. 15, 1978.

Index category: Structural Design.

*Staff Scientist. Associate Fellow AIAA.

face = face sheet of sandwich wall
I = initial rms surface figure error
n = number of circumferential waves in circular element

Introduction

A CONVENTIONAL electromagnetic reflecting system consists of a primary paraboloidal reflecting surface (the "primary"), a relatively small secondary reflecting surface at the focus of the primary (the "secondary"), and a supporting structure that cradles the primary and maintains the position of the secondary at the focus of the primary. The electromagnetic axis (labeled "original axis of revolution" in Fig. 1) is usually aimed by swinging the entire system as a rigid body about an axis perpendicular to the axis of revolution.

The paper is concerned with an unconventional reflecting system: the secondary and its supporting structure and the cradle for the primary are rigidly connected; but as the system is aimed, the primary itself moves and is deformed relative to this cradle while the secondary remains at the focus of the primary and fixed in inertial space. The primary consists of an array of identical elements of circular planform, as shown in Fig. 1. The elements are initially spherical with radius of curvature R. The primary array is reshaped in the following way: each circular element is first positioned as a rigid body by means of actuators for axial displacement and tilt, as indicated in Fig. 2b by the two surfaces S and S''. Each circular element is then deformed or reshaped by edge moment and force actuators distributed around its circumference. In this way the surface, originally spherical with axis of revolution z, becomes to a close approximation paraboloidal with axis of revolution z'. Figure 2a shows the intersection of the original spherical surface with the y,z plane and this intersection after the primary axis of revolution has been retargeted by an angle of α and its surface has been reshaped into a part of a paraboloid. Note that reshapement is needed even if $\alpha=0$, since the original surface is spherical and the reshaped surface must be paraboloidal.

An advantage of a system with a deformable primary over the conventional rigid reflecting system is that it is not necessary to displace the secondary during a maneuver in which the system is aimed in a new direction. Hence, it is possible to design large systems with higher f numbers ($f=R/2D$) without worrying about low-frequency structural dynamic effects associated with a large rotatory inertia. Also, the large primary surface is constructed of relatively small elements, all of which are identical. Hence, it is easier to manufacture the array than it would be if the surface of each of the elements formed a different part of a paraboloid.

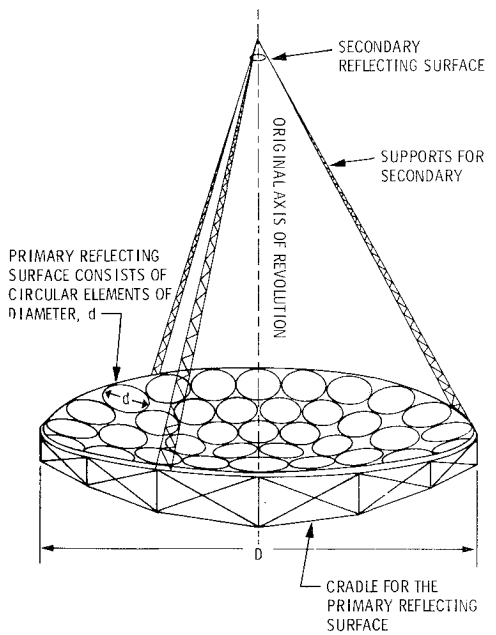

Fig. 1 Large reflecting system with reshapeable primary array.

In this paper the terms "surface error" and "error" are used to denote the difference in the z'' coordinate (Fig. 2b) between the desired surface and the existing surface. "Initial surface error" is the difference $\Delta z''$ between the desired surface and the existing surface after rigid-body alignment of the circular elements but before deformation of them by force and moment actuators which are distributed around their circumferences. "Residual surface error" is the difference $\Delta z''$ between the desired surface and the existing surface after rigid-body alignment and deformation by edge moments and forces. These moments and forces are assumed to be applied by actuators of such a number and arranged around the circumference of each element in such a way that they simulate $\cos n\theta$ variation of the loading. (The results of an investigation of approximately how many actuators are required to do this are included in Ref. 1.)

The purpose of this paper is to derive formulas for the following:

1) Root-mean-squared (rms) difference between the new paraboloidal retargeted surface and the surface of each circular element after rigid-body axial positioning and tilt but before reshaping by edge forces and moments (Fig. 2b).

2) rms residual surface error for each circular element after rigid-body alignment and reshapement.

3) Edge moments and forces required to reshape each circular element.

4) rms surface error of the entire array after rigid-body alignment of the elements but before their reshapement.

5) rms residual surface error of the entire array after reshapement.

These formulas are given in dimensionless forms in terms of the following ratios:

D/λ = (primary array diameter)/(wavelength of electromagnetic radiation)

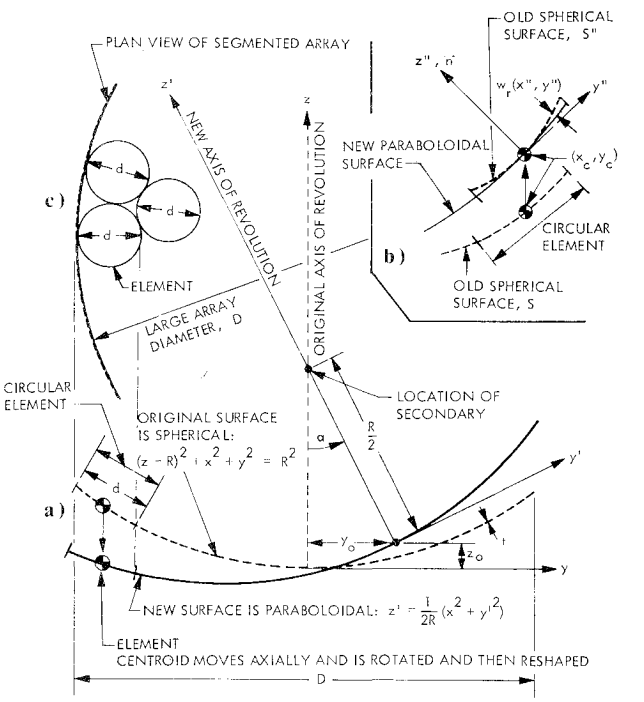

Fig. 2 Rotating the axis of revolution by an angle α while maintaining the focus fixed in inertial space: a) old and new surfaces at the intersection with the y,z plane; b) detail of rigid-body alignment of a single element of the array; c) plan view of a section of the primary array.

D/R = (array diameter)/(original radius of curvature)
d/D = (circular element diameter)/(array diameter)
t/d = (wall thickness)/(circular element diameter)
e = (face sheet thickness)/(total wall thickness)
η^* = dimensionless measure of position of circular element in the primary array (η^* is a function also of the retargeting angle α)

The derivation is based on theories developed by Reissner and his colleagues[2-5] and Flügge.[6] Other work on deformation of reflecting surfaces has been published by Mar and Wan.[7,8]

This paper does not address questions of implementation, such as what types of actuators and control laws should be used for rigid-body alignment of the circular elements or what types of actuators should be used to generate forces and moments around the circumference of each circular element in order to reshape it. It is tacitly assumed that such actuators exist or can be developed. Additional work which bears upon these questions is presented in Refs. 1 and 9.

Required Reshaping

The objective of the derivation of this section is to obtain the displacement distribution $w_r(x'',y'')$ in the z'' direction required for reshapement of a single circular element, as shown in Fig. 2b. The function $w_r(x'',y'')$ represents the difference in z'' between the new paraboloidal surface and the old spherical surface after the element apex at (x_c,y_c) has been moved axially so that it is on the new paraboloidal surface at (x_c,y_c) (see Figs. 2 and 3) and after the element has been tilted about its apex such that the normal to its surface is aligned with the normal $\bar{n}$ to the new paraboloidal surface at (x_c,y_c). The difference $z''_{\text{new}}-z''_{\text{old}}=w_r(x'',y'')$, where subscript r stands for "reshapement," is calculated by writing the equations for the new and old surfaces in the x'',y'',z'' coordinate system, which is associated with the vector triad $\bar{i}'',\bar{j}'',\bar{n}$ shown in Fig. 3. The spherical surface S'' (after rigid-body axial translation and tilting) is expressed in the x'',y'',z'' system as

$$(z''_{\text{old}}-R)^2+x''^2+y''^2=R^2 \tag{1}$$

The paraboloidal surface in the (x',y',z') coordinate system is

$$z'=(1/2R)(x'^2+y'^2) \tag{2}$$

Without loss of generality, the movement of the apex of the retargeted paraboloid as α is increased can be considered to take place in the y,z plane, so that $x'=x$. From Fig. 2a, it is seen that

$$y'=Zs+Yc, \quad z'=Zc-Ys \tag{3}$$

in which

$$c\equiv\cos\alpha, \quad s\equiv\sin\alpha, \quad Z\equiv z-z_0, \quad Y\equiv y-y_0$$

$$y_0=(R/2)s, \quad z_0=(R/2)(1-c) \tag{4}$$

Therefore, in the (x,y,z) system of coordinates the paraboloidal surface is

$$Zc-Ys=(1/2R)[x^2+(Zs+Yc)^2] \tag{5}$$

In order to write Eq. (5) in the (x'',y'',z'') coordinate system, we must use the transformation

$$\begin{Bmatrix} x \\ y \\ z \end{Bmatrix} = \begin{bmatrix} \ell_1 & \ell_2 & \ell_3 \\ m_1 & m_2 & m_3 \\ n_1 & n_2 & n_3 \end{bmatrix} \begin{Bmatrix} x'' \\ y'' \\ z'' \end{Bmatrix} + \begin{Bmatrix} x_c \\ y_c \\ z_c \end{Bmatrix} \tag{6}$$

in which (ℓ_1,ℓ_2,ℓ_3) are the direction cosines of the x axis relative to the (x'',y'',z'') axes, respectively; (m_1,m_2,m_3) are the direction cosines of the y axis relative to (x'',y'',z''), respectively, and (n_1,n_2,n_3) are the direction cosines of the z-axis relative to (x'',y'',z''), respectively. The coordinate systems are shown in Fig. 3. These direction cosines can be derived from an expression for the normal to the new surface at x_c,y_c:

$$\bar{n}=-(\bar{i}\partial f/\partial x+\bar{j}\partial f/\partial y+\bar{k}\partial f/\partial z) \tag{7}$$

in which

$$f\equiv x_c^2+(Z_cs+Y_cc)^2+2R(Y_cs-Z_cc) \tag{8}$$

where

$$Z_c\equiv z_c-z_0 \qquad Y_c\equiv y_c-y_0 \tag{9}$$

and an expression for the tangent plane at x_c,y_c:

$$\bar{n}\cdot(\bar{i}(x-x_c)+\bar{j}(y-y_c)+\bar{k}(z-z_c))=0 \tag{10}$$

The orientation of the vector pair $(\bar{i}'',\bar{j}'')$ can be chosen arbitrarily as long as $\bar{j}''$ is perpendicular to $\bar{i}''$ and both lie in a plane tangent to the new paraboloidal surface at x_c,y_c. If $\bar{i}''$ is chosen such that $y=y_c$ in Eq. (10), we can write

$$\bar{i}''=\bar{i}-(x_c/a)\bar{k} \tag{11}$$

in which

$$a\equiv(Y_cc+Z_cs)s-Rc \tag{12}$$

Furthermore,

$$\bar{j}''=\bar{n}\times\bar{i}'' \tag{13}$$

From Eqs. (7), (11), and (13) and the definitions of the direction cosines given just after Eq. (6), it follows that

$$\ell_1=1/|\bar{i}''|; \quad \ell_2=2x_cb/(a|\bar{j}''|); \quad \ell_3=-2x_c/|\bar{n}| \tag{14a}$$

$$m_1=0; \quad m_2=-2(x_c^2+a^2)/(a|\bar{j}''|); \quad m_3=-2b/|\bar{n}| \tag{14b}$$

$$n_1=-x_c/(a|\bar{i}''|); \quad n_2=2b/|\bar{j}''|; \quad n_3=-2a/|\bar{n}| \tag{14c}$$

in which

$$b\equiv(Y_cc+Z_cs)c+Rs \tag{15}$$

With use of Eq. (5) for the new paraboloidal surface written in the x,y,z coordinate system and the transformation of Eq. (6), one can write the equation for the new surface in the form

$$z''_{\text{new}}=[B''-(B''^2-A''C'')^{1/2}]/A'' \tag{16}$$

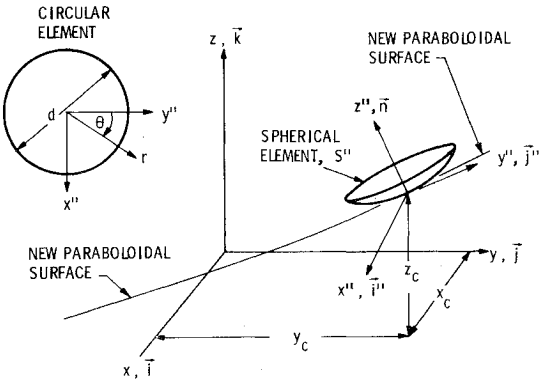

Fig. 3 x'',y'',z'' coordinate system attached to the apex of a circular element after rigid-body alignment.

in which

$$A'' \equiv \ell_3^2 + (cm_3 + sn_3)^2 \tag{17a}$$

$$B'' \equiv -d_1\ell_3 - d_2(cm_3 + sn_3) - R(sm_3 - cn_3) \tag{17b}$$

$$C'' \equiv d_1^2 + d_2^2 + 2Rd_3 \tag{17c}$$

where

$$d_1 \equiv \ell_1 x'' + \ell_2 y'' + x_c \tag{18a}$$

$$d_2 \equiv c(m_1 x'' + m_2 y'' + y_c - y_0) + s(n_1 x'' + n_2 y'' + z_c - z_0) \tag{18b}$$

$$d_3 \equiv s(m_1 x'' + m_2 y'' + y_c - y_0) - c(n_1 x'' + n_2 y'' + z_c - z_0) \tag{18c}$$

The displacement field $w_r(x'',y'')$ is given by

$$w_r(x'',y'') = z''_{\text{new}} - z''_{\text{old}} = \frac{B''}{A''} - \frac{B''}{A''}\left(1 - \frac{A''C''}{B''^2}\right)^{1/2} + R\left(1 - \frac{r^2}{R^2}\right)^{1/2} - R \tag{19}$$

in which

$$r^2 \equiv x''^2 + y''^2 \tag{20}$$

The quantities $A''C''/B''^2$ and $(r/R)^2$ are very small compared to unity, so that the square roots can be expanded, leading to the approximation

$$w_r(x'',y'') \approx \frac{1}{2}\frac{C''}{B''} + \frac{1}{8}\frac{A''C''^2}{B''^3} - \frac{1}{2}R\left(\frac{r}{R}\right)^2 - \frac{1}{8}R\left(\frac{r}{R}\right)^4 - \frac{1}{16}\frac{A''^2C''^3}{B''^5} + \frac{R}{16}\left(\frac{r}{R}\right)^6 \tag{21}$$

From Eqs. (17) with Eqs. (18) and (14), it can be shown, after some algebra, that

$$A'' = r_c'^2/(r_c'^2 + R^2) \tag{22a}$$

$$B'' = e_1 x'' + e_2 y'' + (r_c'^2 + R^2)^{1/2} \tag{22b}$$

$$C'' = a_{11}x''^2 + 2a_{12}x''y'' + a_{22}y''^2 \tag{22c}$$

in which

$$r_c'^2 \equiv x_c^2 + y_c'^2 \tag{23a}$$

$$y_c' \equiv (y_c - y_0)c + (z_c - z_0)s \tag{23b}$$

$$e_1 \equiv x_c^* Rc/[(1 + x_c^{*2})(r_c'^2 + R^2)]^{1/2} \tag{23c}$$

$$e_2 \equiv [Ry_c' + x_c^{*2}(y_c'c + Rs)(y_c's - Rc)] / [(1 + x_c^{*2})^{1/2}(r_c'^2 + R^2)] \tag{23d}$$

$$a_{11} \equiv (1 + s^2 x_c^{*2})/(1 + x_c^{*2}) \tag{23e}$$

$$a_{12} \equiv \{x_c^* c[y_c' + s(y_c's - Rc)x_c^{*2}]\}/[(1 + x_c^2)(r_c'^2 + R^2)^{1/2}] \tag{23f}$$

$$a_{22} \equiv \{R^2 + c^2 x_c^{*2}[y_c'^2 + R^2 - \frac{x_c^{*2}}{1 + x_c^{*2}} \times (y_c'c + Rs)^2]\}/(r_c'^2 + R^2) \tag{23g}$$

where

$$x_c^* \equiv x_c/(y_c's - Rc) \tag{24}$$

The reshapement required for any circular element in the primary array can be obtained from Eq. (21) with Eqs. (22-24) in which x_c is set equal to zero. The reason for this simplification becomes clear after inspection of Fig. 4, recollection that the undeformed circular elements are all spherical and identical, and the following argument: the reshapement required for any circular element with its apex located at a distance r_c' from the axis or revolution z' of the paraboloid is the same except for a phase angle

$$\gamma = \tan^{-1}(x_c/y_c') \tag{25}$$

Since the root-mean-squared initial deviation from the paraboloidal shape and the rms residual error after application of edge loads are independent of this phase angle, these quantities can be calculated with good approximation for the entire array from a knowledge of them at locations in the y,z plane. Given y_c', the locus of points in the x,y plane for which the reshapement requirements are the same (except for phase angle γ) is given by

$$y_c'^2 = x^2 + (1/c^2)(y - y_0 + y_c'^2 s/(2R))^2 \tag{26}$$

The simplifications due to setting $x_c = 0$ in Eqs. (23) lead to

$$A'' = y_c'^2/q^2 \tag{27a}$$

$$B'' = q(1 + Ry_c' r\cos\theta/q^3) \tag{27b}$$

$$C'' = r^2 - (y_c'^2/q^2)r^2\cos^2\theta \tag{27c}$$

where

$$q \equiv (y_c'^2 + R^2)^{1/2} \qquad r \equiv y''\cos\theta \tag{28}$$

In Eq. (21) the last two terms on the right-hand side can be neglected if

$$D\left(\frac{d}{D}\right)^6 \Big/ (32000.f^5) < (\text{allowable residual error}) \tag{29}$$

where D is the diameter of the primary array, d is the diameter of a circular element, and $f = R/(2D)$. It turns out that for reasonable designs the inequality in Eq. (29) is satisfied.

The first two terms on the right-hand side of Eq. (21) are given approximately by

$$\frac{1}{2}\frac{C''}{B''} \approx \frac{r^2}{2q}\left(1 - \frac{y_c'^2}{q^2}\cos^2\theta\right)\left(1 - \frac{Ry_c'}{q^3}r\cos\theta + \left(\frac{Ry_c'}{q^3}\right)^2 r^2\cos^2\theta\ldots\right) \tag{30a}$$

$$\frac{1}{8}\frac{A''C''^2}{B''^3} \approx \frac{y_c'^2 r^4}{8q^5}\left(1 - \frac{y_c'^2}{q^2}\cos^2\theta\right)^2 \tag{30b}$$

in which dots indicate higher-order terms in $(Ry_c'/q^3)^m r^m \cos^m\theta$.

Terms of order

$$\frac{D}{8200}\frac{1}{f^7}\left(\frac{d}{D}\right)^5 \tag{31}$$

have been dropped from Eqs. (30) by truncation of the expansions of $1/B''$ and $1/B''^3$. It turns out that for reasonable designs the quantity in Eq. (31) is negligibly small compared to terms retained.

The reshapement required for any circular element, the apex of which lies in the y,z plane, can be expressed as a trigonometric series,

$$w_r(x'',y'') = w_r(r,\theta) = \sum_{n=0}^{4} g_n(r)\cos n\theta \tag{32}$$

Through use of Eqs. (30) in Eq. (21) and the trigonometric identities,

$$\cos^2\theta = (1+\cos 2\theta)/2 \tag{33a}$$

$$\cos^3\theta = (3\cos\theta+\cos 3\theta)/4 \tag{33b}$$

$$\cos^4\theta = (3/8+\cos 2\theta/2+\cos 4\theta/8) \tag{33c}$$

The following formulas for $g_n(r)$ in Eq. (32) are obtained:

$$g_0(r) = -\frac{r^2}{2}\left(\frac{1}{R}-\frac{1}{q}+\frac{y_c'^2}{2q^3}\right)-\frac{r^4}{8}\left(\frac{1}{R^3}-\frac{y_c'^2}{q^5}-\frac{2R^2y_c'^2}{q^7}+\frac{y_c'^4}{q^7}+\frac{3}{2}\frac{R^2y_c'^4}{q^9}-\frac{3}{8}\frac{y_c'^6}{q^9}\right) \tag{34}$$

$$g_1(r) = \frac{-r^3Ry_c'}{2q^4}\left(1-\frac{3}{4}\frac{y_c'^2}{q^2}\right) \tag{35}$$

$$g_2(r) = \frac{-r^2}{4}\frac{y_c'^2}{q^3}+\frac{r^4}{4}\frac{R^2y_c'^2}{q^7}\left(1-\frac{y_c'^2}{q^2}-\frac{y_c'^2}{2R^2}+\frac{y_c'^4}{4q^2R^2}\right) \tag{36}$$

$$g_3(r) = \frac{r^3}{8}\frac{Ry_c'^3}{q^6} \tag{37}$$

$$g_4(r) = \frac{-r^4}{16}\frac{R^2y_c'^4}{q^9}\left(1-\frac{1}{4}\frac{y_c'^2}{R^2}\right) \tag{38}$$

Deformations Due to Loads at the Edge

The objective of this section is to determine the normal deflections of a shallow spherical cap subjected to normal loads and moments at the edge $r=r_0$, as shown in Fig. 5. In Fig. 5, the moment M and normal force V vary around the circumference as

$$M=\sum_{n=0}^{N} M_n\cos n\theta \quad V=\sum_{n=0}^{N} V_n\cos n\theta \tag{39}$$

The purpose of M and V is to cause the reshapement of each of the circular elements according to Eq. (32). Since the deflections other than rigid-body deflections are very small, linear theory can be used. Hence, the total deformation can be predicted by solution of the problem for each circumferential harmonic and superposition of the resulting normal displacement harmonics:

$$w(r,\theta) = \sum_{n=0}^{N} w_n(r)\cos n\theta \tag{40}$$

Only the $\cos n\theta$ variation of force and displacement are considered because the reshapement required according to Eq. (32) does not contain any $\sin n\theta$ terms.

Axisymmetric Deformations

Reissner[2] derived equations governing the behavior of arbitrarily loaded spherical caps and presented solutions for axisymmetric loading in Ref. 3. For a shallow cap loaded only at the edge, the governing equations are

$$\nabla^2\nabla^2F-\frac{2etE}{R}\nabla^2w=0 \tag{41a}$$

$$-K\nabla^2\nabla^2w+\frac{1}{R}\nabla^2F=0 \tag{41b}$$

in which e is defined later, F is the stress function, K is the flexural rigidity, and the operator ∇ is given by

$$(),_{rr}+\frac{1}{r}(),_r+\frac{1}{r^2}(),_{\theta\theta} \tag{42}$$

In Eq. (42) the subscripts indicate differentiation.

If the spherical cap is closed at its apex and if there is no concentrated load there, the axisymmetric component of the normal displacement field is given by

$$w_0 = C_1\mathrm{ber}(kr)+C_3\mathrm{bei}(kr)+C_2 \tag{43}$$

in which ber and bei are Kelvin functions of order zero [10] and

$$k^4 \equiv C(1-\nu^2)/(KR^2) \tag{44}$$

The quantity C is the extensional rigidity. For sandwich wall construction, the extensional and flexural rigidities are given by

$$C=\frac{2Ete}{1-\nu^2} \qquad K=\frac{eEt^3}{1-\nu^2}\left(\frac{1}{2}-e+\frac{2e^2}{3}\right) \tag{45}$$

where t is the total thickness of the sandwich wall and e is the ratio of the thickness of one face sheet to the total thickness. (Thus, for monocoque wall construction $e=0.5$.) Equations (45) are valid if the extensional rigidity of the core is negligible compared to C, as is the case with honeycomb material. The meridional bending moment at the edge of the axisymmetrically loaded shallow spherical cap is

$$M_0 = Kk^2\{C_1[\mathrm{bei}(kr_0)+(1-\nu)\mathrm{ber}'(kr_0)/(kr_0)] + C_3[\mathrm{ber}(kr_0)-(1-\nu)\mathrm{bei}'(kr_0)/(kr_0)]\} \tag{46}$$

and the meridional stress resultant N_0 is

$$N_0 = Ct\left(\frac{1-\nu^2}{12}\right)^{1/2}k^2[C_1\mathrm{bei}'(kr_0)-C_3\mathrm{ber}'(kr_0)]/(kr_0) \tag{47}$$

In Eqs. (46) and (47), superscript prime indicates differentiation with respect to (kr). The undetermined constants C_1 and C_3 can be obtained for a free cap loaded at the edge by a unit moment by setting $N_0=0$ and $M_0=1$. Equilibrium of axial forces requires that the transverse load V_0 be zero at $r=r_0$. The constant C_2 in Eq. (43) represents, within the accuracy of Reissner's formulation, the rigid-body displacement of the cap in the axial (z'') direction.

In the derivation of the minimum mean-squared residual surface figure error for $n=0$, the axisymmetric displacement field caused by an edge moment M_0 plus the rigid-body axial displacement is given by

$$w_0 = C_1\left[\mathrm{ber}(kr)+\left(\frac{\mathrm{bei}'(kr_0)}{\mathrm{ber}'(kr_0)}\right)\mathrm{bei}(kr)\right]+C_2\left[1-\left(\frac{r}{R}\right)^2\right]^{1/2} \tag{48}$$

The last term on the right-hand side of Eq. (48) is a more accurate representation of the rigid-body displacement than that given in Eq. (43). The constants C_1 and C_2 are calculated

such that the mean-squared difference between w_0 in Eq. (48) and g_0 in Eq. (34) is minimized. The edge moment M_0 required to achieve this minimized error is then calculated from Eq. (46), with

$$C_3 = C_1 \text{bei}'(kr_0)/\text{ber}'(kr_0) \tag{49}$$

which results from the condition $N_0 = 0$ at r_0.

For practical designs the argument kr is small enough to permit use of the following asymptotic expansions for the Kelvin functions:

$$\text{ber}(kr) = 1 - y^2/(2!)^2 + y^4/(4!)^2 - \ldots \tag{50a}$$

$$\text{bei}(kr) = y - y^3/(3!)^2 + y^5/(5!)^2 - \ldots \tag{50b}$$

in which

$$y \equiv k^2 r^2/4 \tag{51}$$

Solution for $n = 1$ Circumferential Wave

Reissner[4] obtained solutions of Eqs. (41) for nonsymmetric loading. In particular, for $n = 1$ circumferential wave, the normal displacement for a cap closed at the apex is given by

$$w_1(r,\theta) = [C_1 J_1(z) + C_3 I_1(z) + C_2 r]\cos\theta \tag{52}$$

where J_i and I_i denote Bessel functions of order i and the complex variable z is given by

$$z \equiv (i)^{1/2} kr \tag{53}$$

The edge moment M_1 is

$$M_1 = iKk^2\{C_1[J_3(z_0) - (3+\nu)J_2(z_0)/z_0] + C_3[I_3(z_0) + (3+\nu)I_2(z_0)/z_0]\}\cos\theta \tag{54}$$

and the boundary condition $N_1 = 0$ at $r = r_0$ yields

$$C_1[-4J_3/z_0 + J_2(1 + 16/z_0^2) - 4J_1/z_0] + C_3[-4I_3/z_0 + I_2(1 - 16/z_0^2) + 4I_1/z_0] = 0 \tag{55}$$

with the Bessel functions J_i, I_i being evaluated at

$$z = z_0 = (i)^{1/2} kr_0 \tag{56}$$

The displacement field caused by an edge moment M_1 plus the rigid-body tilt about $\theta = \pi/2$ is given by

$$w_1(r) = C_1[J_1(z) + C_0 I_1(z)] + C_2 r \tag{57}$$

in which $C_0 = C_3/C_1$ [obtained from Eq. (55)].

The constants C_1 and C_2 are calculated such that the mean-squared difference between $w_1(r)$ in Eq. (57) and g_1 in Eq. (35) is minimized. The edge moment M_1 required to achieve this minimized error is then calculated from Eq. (54) with C_3 being calculated from Eq. (55).

For practical designs the argument z is small enough to permit use of the following asymptotic expansions for the Bessel functions:

$$J_n(z) = \left(\frac{1}{2}z\right)^n \sum_{k=0}^{\infty} \frac{(-y)^k}{k!(n+k)!} \tag{58a}$$

$$I_n(z) = \left(\frac{1}{2}z\right)^n \sum_{k=0}^{\infty} \frac{(+y)^k}{k!(n+k)!} \tag{58b}$$

in which

$$y \equiv z^2/4 \tag{59}$$

In order that the free cap remain in equilibrium under the edge moment M_1, there must exist a normal reaction at the edge:

$$V_1 = \frac{M_1}{r_0} = Q_1 + \frac{1}{r_0}\frac{\partial M_{r\theta}}{\partial \theta} \tag{60}$$

where Q_1 is the transverse shear resultant and $M_{r\theta}$ is the twisting moment resultant.

Solution for $n \geq 2$ Circumferential Waves

The problem of general nonsymmetric deformations of spherical caps loaded at the edge could be solved with use of Reissner's equations (41) which yield normal displacement fields analogous to that given in Eq. (52). Such an analysis would lead to values of edge moment resultant M_n and normal force resultant V_n that minimize the mean-squared residual surface error in the nth circumferential harmonic. An independent numerical analysis[9] in which M_n and V_n are derived without any restrictions on the displacement field yields values for M_n and V_n that closely correspond to those predicted with the assumption of inextensional bending. Therefore, the assumption of inextensional bending for $n \geq 2$ is made here. Johnson and Reissner[5] studied inextensional bending of shallow spherical caps. Flügge[6] derived equations for inextensional bending of spherical shells of any depth. Wan[11] determined that if $[r_0/(Rt)^{1/2}][12(1-\nu^2)]^{1/4} \gg n > 1$, the state in the interior of an edge-loaded shallow spherical shell is adequately predicted with use of inextensional bending theory.

The normal displacement field for inextensional bending of a spherical cap closed at the apex is given by Flügge[6] as

$$w_n(r,\theta) = C_n(n + \cos\phi)\tan^n(\phi/2)\cos n\theta \tag{61}$$

The polar angle ϕ is shown in Fig. 5.

The meridional moment corresponding to this inextensional displacement field is

$$M_n = \frac{C_n K(1-\nu)n(n^2-1)}{R^2}\frac{\tan^n(\phi/2)}{\sin^2\phi}\cos n\theta \tag{62}$$

The inextensional bending field leads to

$$N_n = Q_n = 0 \tag{63a}$$

$$V_n = Q_n + \frac{1}{r}\frac{\partial M_{r\theta n}}{\partial \theta} = -\frac{n}{r}M_n \tag{63b}$$

The constant C_n in Eq. (61) is calculated such that the mean-squared difference between $w_n(r)$ in Eq. (61) and g_2 or g_3 or g_4 in Eqs. (36-38), respectively, is minimized. The edge moment M_n required to achieve this minimized error is then calculated from Eq. (62).

For practical designs the argument ϕ is small enough to permit use of the following relationships:

$$\tan(\phi/2) = \tfrac{1}{2}(r/R)[1 + \tfrac{1}{4}(r/R)^2] \tag{64a}$$

$$n + \cos\phi = n + 1 - \tfrac{1}{2}(r/R)^2 \tag{64b}$$

$$w_n(r) = C_n\left[\frac{1}{2}\left(\frac{r}{R}\right)\right]^n\left\{n + 1 + \left[\frac{n(n+1)}{4} - \frac{1}{2}\right]\left(\frac{r}{R}\right)^2\right\} \tag{64c}$$

Mean-Squared Residual Surface Error

The total mean-squared residual surface error of a single circular element of the primary array is the sum of the mean-squared residual errors for each of the circumferential harmonics $n = 0$ through 4. For each harmonic the mean-squared

error over a circular element is

$$E_n^2 = \frac{1}{\pi r_0^2}\int_0^{2\pi}\int_0^{r_0}(w_n - g_n)^2\cos^2 n\theta r\,dr\,d\theta \tag{65}$$

$$= \frac{A}{r_0^2}\int_0^{r_0}(w_n - g_n)^2 r\,dr \tag{66}$$

in which $A=2$ if $n=0$ and $A=1$ if $n>0$. For $n=0$ and $n=1$ the functions $w_0(r)$ and $w_1(r)$ each contain two undetermined coefficients, C_1 and C_2, as seen in Eqs. (48) and (57). These coefficients are determined by setting

$$\frac{\partial(E_n^2)}{\partial C_1} = \frac{\partial(E_n^2)}{\partial C_2} = 0 \tag{67}$$

This minimization of the mean-squared error E_n with respect to C_1 and C_2 yields

$$C_1 = (a_{22}b_1 - a_{12}b_2)/(a_{11}a_{22} - a_{12}^2) \tag{68a}$$

$$C_2 = (a_{11}b_2 - a_{12}b_1)/(a_{11}a_{22} - a_{12}^2) \tag{68b}$$

in which

$$a_{11} \equiv \int_0^{r_0} f_1^2 r\,dr, \quad a_{12} \equiv \int_0^{r_0} f_1 f_2 r\,dr$$

$$a_{22} \equiv \int_0^{r_0} f_2^2 r\,dr, \quad b_1 \equiv \int_0^{r_0} g_n f_1 r\,dr$$

$$b_2 \equiv \int_0^{r_0} g_n f_2 r\,dr \tag{69}$$

where the displacement field w_n has been taken to be

$$w_n(r) = C_1 f_1(r) + C_2 f_2(r) \tag{70}$$

Corresponding to the values of C_1 and C_2 given in Eqs. (68), it can be shown that the mean-squared residual surface error is

$$E_n^2 = \frac{A}{r_0^2}\left[-C_1 b_1 - C_2 b_2 + \int_0^{r_0} g_n^2 r\,dr\right] \tag{71}$$

If there is only one undetermined constant, as is the case for $n \geq 2$,

$$E_n^2 = \frac{A}{r_0^2}\left[-C_n b_1 + \int_0^{r_0} g_n^2 r\,dr\right] \tag{72}$$

in which

$$C_n = b_1/a_{11} \tag{73}$$

Calculation of the residual error is straightforward. The functions f_1 and f_2 are obtained from Eqs. (48) with the asymptotic expansions of Eq. (50), from Eq. (57) with the asymptotic expansions of Eqs. (58), and from Eq. (64c). The functions g_n are obtained from Eqs. (34-38). In the cases $n=0$ and $n=1$, derivation of formulas for the residual errors is extremely tedious, since three terms in the asymptotic expansions must be retained during the algebraic manipulations in order to obtain the correct results. These manipulations involve products of integrals as seen from Eq. (68), integrals of products as seen from Eq. (69), and quotients as seen from Eqs. (49), (57), and (68). Therefore, the formulas for rms residual error for $n=0$ and $n=1$, given in the next section as Eqs. (79) and (82), represent the final results after many pages of algebra.

Approximate Formulas for the Initial and Residual Errors and Edge Moments for $n=0, 1, 2, 3, 4$ Circumferential Waves

For small retargeting angles α and shallow primary arrays, y_c' in Fig. 4 is approximately given by

$$y_c' \approx \frac{D}{2}\left(\eta - \frac{R}{D}\alpha\right) = \frac{D}{2}\eta^* \tag{74}$$

in which

$$\eta \equiv 2y_c/D \quad -1 \leq \eta \leq +1 \tag{75}$$

In addition, since $y_c' < R$, the quantity q^m which appears in Eqs. (34-38) can be expanded thus,

$$q^m = (y_c'^2 + R^2)^{m/2} = R^m\left(1 + \frac{m}{2}\frac{y_c'^2}{R^2} + \ldots\right) \tag{76}$$

Many of the higher-order terms in y_c'/q, particularly those multiplied by r^4 in Eqs. (34) and (36), can be dropped.

Formulas for the initial and residual rms surface error are to be given for each circumferential harmonic. The initial surface error (error before reshapement) in the nth circumferential harmonic is defined as

$$E_{In}^2 = \frac{A}{r_0^2}\int_0^{r_0} g_n^2 r\,dr \tag{77}$$

The root-mean squared surface errors are given by E_{In} and E_n. The following formulas for the root-mean-squared error are written in dimensionless form in terms of design parameters of the problem, D/λ, D/R, d/D, t/d, e, and η^* defined earlier.

$n=0$ Circumferential Waves

$$\frac{E_{I0}}{\lambda} = \frac{1}{64\sqrt{3}}\frac{D}{\lambda}\eta^{*2}\left(\frac{d}{D}\right)^2\left(\frac{D}{R}\right)^3\left[1 - \frac{9}{32}\left(\frac{D}{R}\right)^2\eta^{*2}\right] \tag{78}$$

$$\frac{E_0}{\lambda} = 1.52\times 10^{-6}\frac{D}{\lambda}\left(\frac{d}{D}\right)^4\left(\frac{D}{R}\right)^3 \times\left[\frac{(D/R)^2\eta^{*2}(d/t)^2(1-\nu^2)}{(0.5 - e + 2e^2/3)} - 384\right] \tag{79}$$

$$\frac{M_0}{ED^2} = \frac{-e(0.5 - e + 2e^2/3)}{4(1-\nu)}\left(\frac{t}{d}\right)^3\left(\frac{D}{R}\right)^3\left(\frac{d}{D}\right)^3 \times\left[\eta^{*2}\left\{1 - \frac{9}{32}\left(\frac{D}{R}\right)^2\eta^{*2}\right\} + \frac{1}{4}\left(\frac{d}{D}\right)^2\right] \tag{80}$$

$n=1$ Circumferential Wave

$$\frac{E_{I1}}{\lambda} = \frac{1}{32\sqrt{8}}\frac{D}{\lambda}|\eta^*|\left(\frac{d}{D}\right)^3\left(\frac{D}{R}\right)^3\left[1 - \frac{11}{16}\left(\frac{D}{R}\right)^2\eta^{*2}\right] \tag{81}$$

$$\frac{E_1}{\lambda} = \frac{5.76\times 10^{-5}}{2^8}\frac{D}{\lambda}|\eta^*| \times\left[\left(\frac{D}{R}\right)^5\left(\frac{d}{t}\right)^2\left(\frac{d}{D}\right)^5(1-\nu^2)\right]\Big/(0.5 - e + 2e^2/3) \tag{82}$$

$$\frac{M_1}{ED^2} = \frac{-e(0.5 - e + 2e^2/3)}{4(1-\nu^2)}\left(\frac{t}{d}\right)^3\left(\frac{D}{R}\right)^3\left(\frac{d}{D}\right)^4\eta^* \times\left[1 - \frac{11}{16}\left(\frac{D}{R}\right)^2\eta^{*2}\right] \tag{83}$$

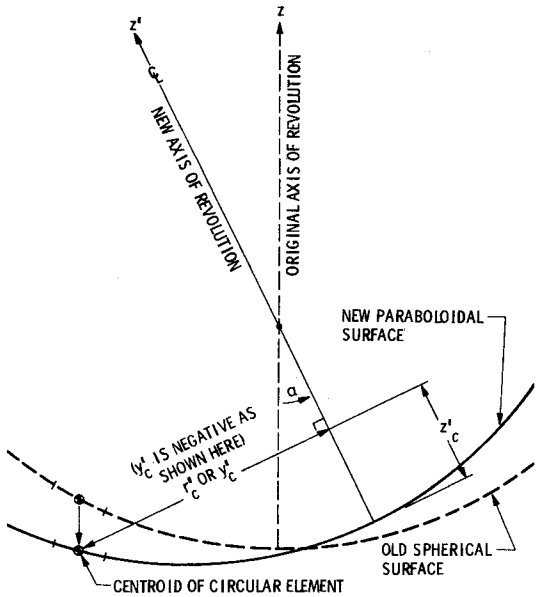

Fig. 4 Old and new surfaces showing the quantities r'_c, y'_c, and z'_c.

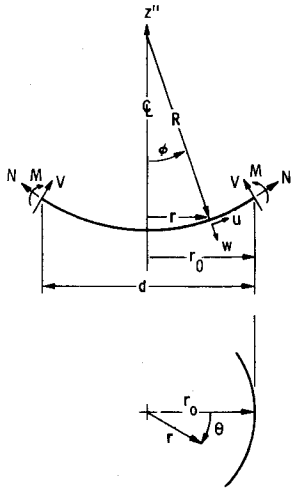

Fig. 5 Coordinates, displacements, and edge force and moment resultants for circular element.

$n=2$ Circumferential Waves

$$\frac{E_{I2}}{\lambda}=\frac{1}{64\sqrt{6}}\frac{D}{\lambda}\eta^{*2}\left(\frac{d}{D}\right)^2\left(\frac{D}{R}\right)^3\left[1-\frac{3}{8}\left(\frac{D}{R}\right)^2\eta^{*2}\right] \tag{84}$$

$$\frac{E_2}{\lambda}=\frac{1}{768\sqrt{10}}\frac{D}{\lambda}\eta^{*2}\left(\frac{d}{D}\right)^4\left(\frac{D}{R}\right)^5 \tag{85}$$

$$\frac{M_2}{ED^2}=\frac{-e(0.5-e+2e^2/3)}{8(1+\nu)}\left(\frac{t}{d}\right)^3\left(\frac{D}{R}\right)^3\left(\frac{d}{D}\right)^3\eta^{*2}\times\left[1-\frac{3}{8}\left(\frac{D}{R}\right)^2\eta^{*2}\right] \tag{86}$$

$n=3$ Circumferential Waves

$$\frac{E_{I3}}{\lambda}=\frac{1}{512\sqrt{8}}\frac{D}{\lambda}|\eta^{*3}|\left(\frac{d}{D}\right)^3\left(\frac{D}{R}\right)^5\left[1-\frac{3}{4}\left(\frac{D}{R}\right)^2\eta^{*2}\right] \tag{87}$$

$$\frac{E_3}{\lambda}=\frac{1}{32768\sqrt{3}}\frac{D}{\lambda}|\eta^{*3}|\left(\frac{d}{D}\right)^5\left(\frac{D}{R}\right)^7 \tag{88}$$

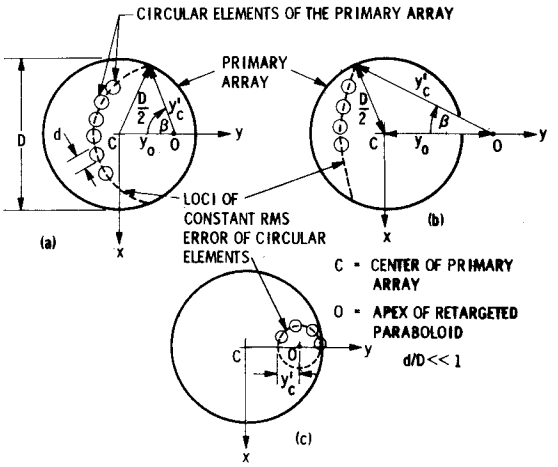

Fig. 6 Loci of constant rms initial and residual surface error for circular elements in the large primary array.

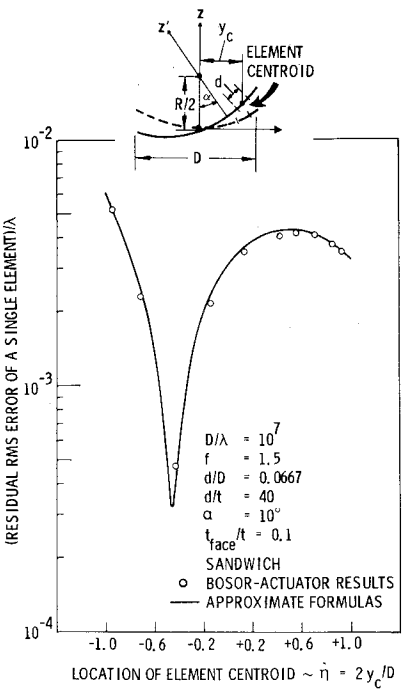

Fig. 7 Comparison of rms residual surface error calculated from the analysis presented in this paper and from the analysis of Ref. 9.

$$\frac{M_3}{ED^2}=\frac{3e(0.5-e+2e^2/3)}{64(1+\nu)}\left(\frac{t}{d}\right)^3\left(\frac{D}{R}\right)^5\left(\frac{d}{D}\right)^4\eta^{*3}\times\left[1-\frac{3}{4}\left(\frac{D}{R}\right)^2\eta^{*2}\right] \tag{89}$$

$n=4$ Circumferential Waves

$$\frac{E_{I4}}{\lambda}=\frac{1}{4096\sqrt{10}}\frac{D}{\lambda}\eta^{*4}\left(\frac{d}{D}\right)^4\left(\frac{D}{R}\right)^7 \tag{90}$$

$$\frac{E_4}{\lambda}=\frac{E_{I4}}{\lambda} \tag{91}$$

$$M_4=0 \tag{92}$$

There was not attempt to correct the $n=4$ component of surface error in Eq. (90) as it is small.

Inspection of the formulas for surface error reveals some interesting facts:

1) The influence of shell wall thickness on residual surface error affects only the $n=0$ and $n=1$ modes.

2) For primary reflectors with reasonable element diameter-to-thickness ratios d/t, the axisymmetric residual error E_0/λ dominates.

3) The initial rms error for $n \geq 2$ is given approximately by

$$\frac{E_n}{\lambda} = \frac{1}{8^n (2n+2)^{1/2}} \frac{D}{\lambda} \eta^{*n} \left(\frac{d}{D}\right)^n \left(\frac{D}{R}\right)^{2n-1} \tag{93}$$

This formula can be used to calculate the highest n for which error control by edge forces is required.

4) Since the axisymmetric component of residual rms error dominates, the residual error for a primary reflector of sandwich construction is approximately equal to that of monocoque construction providing that the following equation is satisfied:

$$\left(\frac{d}{t}\right)^2_{\text{sandwich}} = (3-6e+4e^2)\left(\frac{d}{t}\right)^2_{\text{monocoque}} \tag{94}$$

Thus, for given values of all other variables, the thickness of a sandwich wall can be less than that for a monocoque wall.

The total mass of the primary reflector is given by

$$\text{Total Primary Mass} = \frac{\pi}{4} \rho_{\text{face}} D^3 \left(\frac{t}{d}\right)\left(\frac{d}{D}\right) \times \left[2e + \frac{\rho_{\text{core}}}{\rho_{\text{face}}}(1-2e)\right] \tag{95}$$

It is generally true that $\rho_{\text{core}}/\rho_{\text{face}} < 1$. Because of Eqs. (94) and (95), and since smaller edge moments and forces are required for reshaping sandwich walls than monocoque walls of a given d/t, it is clearly advantageous to use sandwich construction for the primary reflector.

Calculation of Initial and Residual Errors for Entire Primary Array

Figure 6 shows a plan view of the primary array with center at C and apex of the retargeted parabola at 0. The dotted line is a circle with radius y_c', which for small retargeting angles α and shallow primary arrays is given approximately by Eq. (74). This dotted line represents, to the same degree of approximation, the locus of points in the x,y plane associated with a constant element surface error. Such a locus is obtained from Eq. (26) by setting $c^2 = 1$ and dropping $y_c'^2 s/(2R)$ compared to $y - y_0$. If the apex of the retargeted primary lies within the array, the mean-squared error of the entire array is given by

$$E^2 = \frac{4}{\pi D^2} \int_0^{D/2+y_0} 2 \sum_{n=0}^{4} E_n^2 y_c' \beta \, dy_c' \tag{96}$$

This integral can be divided into two parts,

$$E^2 = \frac{4}{\pi D^2} \left[2\pi \int_0^{D/2-y_0} \sum_{n=0}^{4} E_n^2 y_c' \, dy_c' + 2 \int_{D/2-y_0}^{D/2+y_0} \sum_{n=0}^{4} E_n^2 y_c' \beta \, dy_c'\right] \tag{97}$$

in which

$$\beta = \cos^{-1}\left[\frac{y_c'^2 + y_0^2 - (D/2)^2}{2 y_c' y_0}\right] \tag{98}$$

The first integral on the right-hand side of Eq. (97) corresponds to loci such as shown in Fig. 6c and the second to loci such as shown in Fig. 6a. If the apex 0 of the retargeted primary lies outside of the array, such as shown in Fig. 6b, the mean-squared error of the entire array is given by

$$E^2 = \frac{4}{\pi D^2} \int_{y_0-D/2}^{y_0+D/2} \sum_{n=0}^{4} E_n^2 y_c' 2\beta \, dy_c' \tag{99}$$

In Eqs. (97) and (99) E_n^2 denotes the mean-squared error of a circular element for n circumferential waves.

In calculations of the mean-squared errors of the entire array, the second integration on the right-hand side of Eq. (97) and the integration in Eq. (99) are performed numerically by Simpson's rule. The analysis of this section is valid only if the diameter d of a circular element is small compared to the diameter D of the primary array.

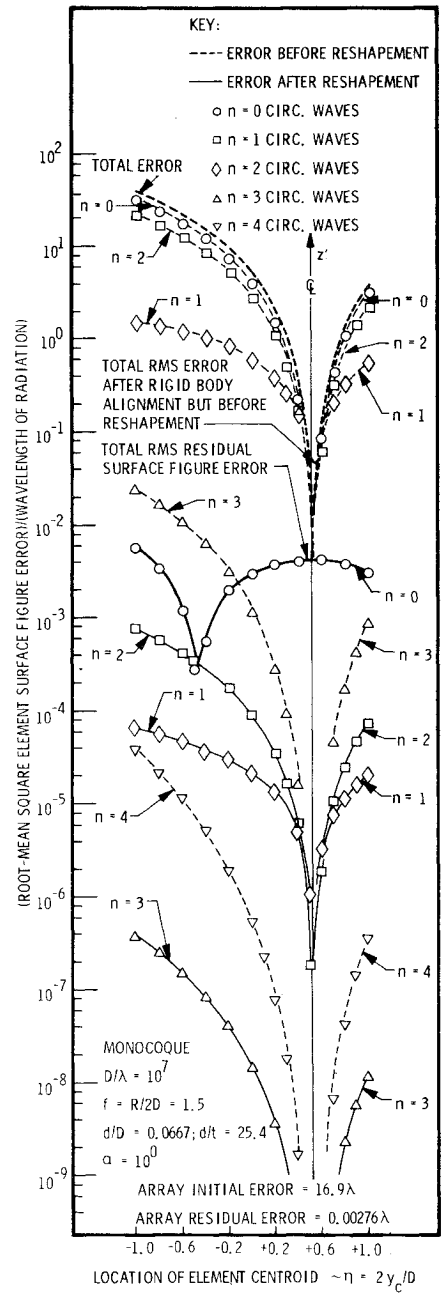

Fig. 8 Initial and residual rms surface errors for various circumferential wavenumbers n as a function of position of the circular element in the primary array.

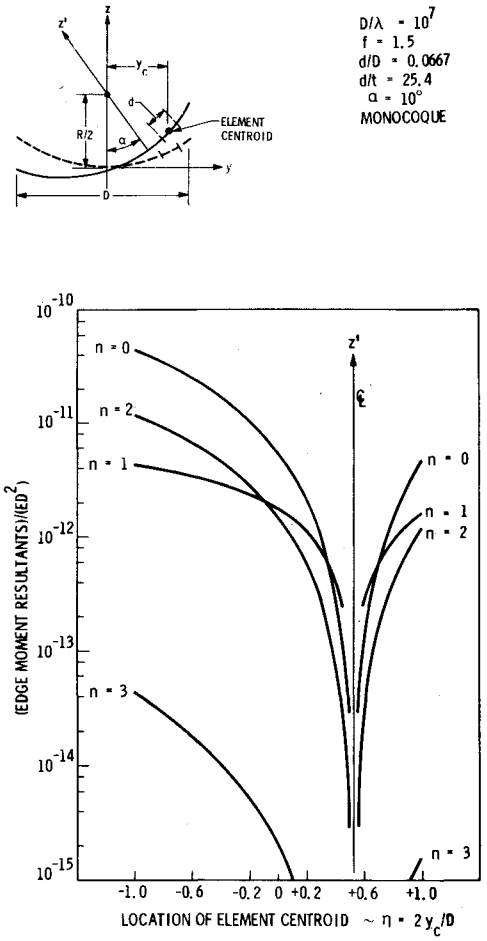

Fig. 9 Edge moment resultant amplitudes required for minimization of rms residual surface error in a circular element as a function of position of this element in the primary array.

Numerical Results

Figures 7-9 show some results of application of Eqs. (78-90) to a system with $D/\lambda = 10^7$, which would most likely apply to an optical reflector. Figure 7 gives the rms residual error vs η of a single circular element. The solid line corresponds to the rms error predicted from the square root of the sum of the squares of the right-hand sides of Eqs. (79, 82, 85, 88, and 91). The points correspond to results obtained from a computer program, BOSOR-ACTUATOR, based on the numerical method presented in Ref. 9. The analysis of Ref. 9 does not contain any limitations from shallow shell theory nor approximations such as defined by Eqs. (50, 58, 64, 74, and 76). In the BOSOR-ACTUATOR analysis, displacement influence functions corresponding to actuator edge moments and forces given by Eqs. (39) are obtained by BOSOR from a finite-difference energy technique valid for any shell of revolution. Calculation of the rms surface error is performed by ACTUATOR, in which quantities such as defined by Eqs. (69) are derived by numerical integration. The displacement distribution required for reshapement, $w_r(r,\theta)$, is generated in ACTUATOR by Fourier series expansions of the circumferential variations at several radial stations and radial variation by least-squares polynomial fitting of the Fourier coefficients. Since the essentially numerical analysis of Ref. 9 and the "closed-form" analysis presented here are so dissimilar, the agreement of the two indicated in Fig. 7 tends to validate both.

Figure 8 shows the initial and residual rms errors E_{In} and E_n of a circular element located at various η. All curves in Fig. 8 are symmetric about the z' axis. Note that, except for elements located in the neighborhood of $\eta = -4.5$, the residual error is essentially axisymmetric. Actuation of the elements in the immediate neighborhood of y'_0, the intersection of the new axis of revolution with the surface of the retargeted paraboloid, is relatively ineffective in correcting the small initial error there because an axisymmetric edge moment does not transform a shallow spherical cap into a shallow paraboloidal cap, but merely changes its radius of curvature uniformly. The dip near $\eta = -4.5$ in the curve for total rms residual error of an element occurs because the term in brackets in Eq. (79) for the axisymmetric component of residual error vanishes near $\eta = -4.5$ in this particular case.

Figure 9 gives the amplitude of the edge moment resultants M_n as a function of circular element location η for the same case as that from which Fig. 8 is derived. For elements located equidistant from the new axis of symmetry (z' axis) but on opposite sides of it, the circumferential distributions of moments corresponding to even values of n are the same and those for odd values of n are of opposite sign. The normal force resultants V_n are obtained from Eqs. (60) and (63).

Conclusions

The purpose of this paper is to derive the formulas for initial and residual rms surface error and edge moment amplitude given in Eqs. (78-92). These formulas apply to the aiming of shallow primary reflectors in such a way that the secondary reflector does not translate. The edge moment and force resultants required to minimize the rms residual surface error are derived for $n=0$ and $n=1$ circumferential waves from a shallow shell theory published by Reissner in 1946[2] and for $n \geq 2$ circumferential waves from an inextensional bending theory published by Flügge in 1960.[6]

Other numerical results pertinent to the design of an optical system are presented in a comparison paper.[1] There, the ratios d/t and d/D are calculated for various f numbers such that the rms residual error for the entire array is less than 0.01 times the wavelength of electromagnetic radiation. The corresponding maximum actuator moments and the total mass of the primary array are plotted for monocoque and sandwich wall construction. The dependence of rms initial and residual error on retargeting angle α is shown. Finally, in Ref. 1 the analysis of Ref. 9 is used to determine the additional rms residual surface error induced because the actuator forces and moments would in reality be applied at discrete points on the circumference of each circular element rather than as smooth functions, $\cos n\theta$, as assumed in Eqs. (39).

Acknowledgment

This research was supported by the 1978 Lockheed Independent Research and Independent Development Programs.

References

[1] Bushnell, D., "Aiming an Electromagnetic Beam by Bending the Segments of a Large Reflecting Surface: A Parameter Study," *Proceedings of Symposium Honoring Professor Eric Reissner*, University of California, San Diego, Calif., June 23, 1978; to appear in *Mechanics Today*, Vol. 5, edited by S. Nemat-Nasser, Pergamon Press, 1979 or 1980.

[2] Reissner, E., "Stresses and Small Displacements of Shallow Spherical Shells, I," *Journal of Mathematical Physics*, Vol. 25, 1946, pp. 80-85.

[3] Reissner, E., "Stress and Small Displacements of Shallow Spherical Shells, II," *Journal of Mathematical Physics*, Vol. 25, 1946, pp. 279-300; corrections in Vol. 27, 1948, p. 240.

[4] Reissner, E., "On the Determination of Stresses and Displacements for Unsymmetrical Deformations of Shallow Spherical Shells," *Journal of Mathematical Physics*, Vol. 38, 1959, pp. 16-35.

[5]Johnson, M. W. and Reissner, E., "On Inextensional Deformations of Shallow Elastic Shells," *Journal of Mathematical Physics*, Vol. 34, 1955, pp. 335-346.

[6]Flügge, W., *Stresses in Shells*, Springer-Verlag, Berlin, 1960, pp. 386-387.

[7]Mar, J. W. and Wan, F.Y.M., "The Influence of Shell Behavior on the Design of Large Antennas," *Proceedings of the 16th International Astronautical Congress*, Athens, Greece, 1965, pp. 183-212.

[8]Mar, J. W. and Wan, F.Y.M., "The Use of Sandwich Shells in Large Steerable Aerials," *Proceedings of the Conference on Large Steerable Aerials for Satellite Communication, Radio Astronomy and Radar, Design and Construction of Large Steerable Aerials,* IEE Conference Publication 21, London, 1966, pp. 125-129.

[9]Bushnell, D., "Control of Surface Configuration by Application of Concentrated Loads," *AIAA Journal*, Vol. 17, Jan. 1979, pp. 71-77; also "Control of Surface Configuration of Nonuniformly Heated Shells," *AIAA Journal*, Vol. 17, Jan. 1979, pp. 78-84.

[10]Abramowitz, M. and Stegun, I. A., (Eds.), *Handbook of Mathematical Functions*, U.S. Dept. of Commerce Applied Mathematics Ser. 55, third printing, March 1965, Chap. 9, pp. 358-385.

[11]Wan, F.Y.M., "Membrane and Bending Stresses in Shallow Spherical Shells," *International Journal of Solids and Structures*, Vol. 3, 1967, pp. 353-366.